Crystal Structure of the Soluble Form of Equinatoxin II, a Pore-Forming Toxin from the Sea Anemone *Actinia equina*

Alekos Athanasiadis,*§ Gregor Anderluh,†
Peter Maček,† and Dušan Turk*‡
*Department of Biochemistry
   and Molecular Biology
Jozef Stefan Institute
Jamova 39
1000 Ljubljana
Slovenia
†University of Ljubljana
Biotechnical Faculty
Department of Biology
Večna pot 111
1000 Ljubljana
Slovenia

Summary

Background: Membrane pore–forming toxins have a remarkable property: they adopt a stable soluble form structure, which, when in contact with a membrane, undergoes a series of transformations, leading to an active, membrane-bound form. In contrast to bacterial toxins, no structure of a pore-forming toxin from an eukaryotic organism has been determined so far, an indication that structural studies of equinatoxin II (EqtII) may unravel a novel mechanism.

Results: The crystal structure of the soluble form of EqtII from the sea anemone *Actinia equina* has been determined at 1.9 Å resolution. EqtII is shown to be a single-domain protein based on a 12 strand β sandwich fold with a hydrophobic core and a pair of α helices, each of which is associated with the face of a β sheet.

Conclusions: The structure of the 30 N-terminal residues is the largest segment that can adopt a different structure without disrupting the fold of the β sandwich core. This segment includes a three-turn α helix that lies on the surface of a β sheet and ends in a stretch of three positively charged residues, Lys-30, Arg-31, and Lys-32. On the basis of gathered data, it is suggested that this segment forms the membrane pore, whereas the β sandwich structure remains unaltered and attaches to a membrane as do other structurally related extrinsic membrane proteins or their domains. The use of a structural data site-directed mutagenesis study should reveal the residues involved in membrane pore formation.

Introduction

Equinatoxin II (EqtII) from the sea anemone *Actinia equina* is classified as a sphingomyelin-inhibited actino-

‡To whom correspondence should be addressed (e-mail: dusan.turk@ijs.si).
§Present address: Massachusetts Institute of Technology, Department of Biology, 68-247, 77 Massachusetts Avenue, Cambridge, Massachusetts, 02139.

porin, a transmembrane solute transporter belonging to the pore-forming equinatoxin family 1.C.38 [1]. The sequence of EqtII is very similar to that of Tenebrosin-C from *Actinia tenebrosa* and shows about 60% identity to Sticholysins I and II from *Stichodactyla helianthus* and the lysin from *Heteractis magnifica* [2]. EqtII is a cytolytic water-soluble protein that readily associates with cell and artificial lipid membranes [3–5]. In membranes, without the involvement of a specific receptor, 3–4 EqtII monomers oligomerize and create cation-selective pores that are ∼2 nm in inner diameter [5]. EqtII is strongly cytolytic [6] and lethal due to its cardiotoxic effects [7].

The understanding of the mechanisms of membrane pore formation induced by toxins is based mainly on structural studies of bacterial proteins. In the process of membrane binding and insertion, these proteins undergo a series of changes in structure, solubility, and oligomerization state (reviewed in [8]). Three mechanisms by which toxins insert into membranes have been reported: penetration by helices [9, 10], penetration by a β barrel comprised of β hairpins (one from each monomer [11, 12]), or by transformation of a helical structure into β hairpins, which insert into the membrane upon binding [13].

In contrast to bacterial pore-forming toxins, no three-dimensional structure of such a protein from eukaryotic organisms has been determined at the atomic level. The crystal structure of EqtII presented here, solved by MIR methods and refined against data at 1.9 Å resolution, reveals the fold of the family and allows the mechanism of structural reorganization on membrane insertion to be addressed.

Results and Discussion

Overall Structure and Fold

The final model comprises 174 out of 179 amino acid residues. Residues are numbered consecutively (from Ala-5 to Ala-179) in accordance with the amino acid sequence of mature EqtII [14]. The asymmetric unit of the crystal contains two molecules that are related by a noncrystallographic dyad with an rmsd of 0.25 Å calculated over 161 Cα atom pairs of equivalent residues. A single EqtII molecule fits into a box of 42 × 28 × 32 Å.

The EqtII molecule is a single-domain structure. The fold is based on a β sandwich (Figure 1a–d) with six β strands in each sheet. The strands at the edges are short. A helix is associated with the face of each β sheet. The secondary structure elements are addressed as shown in Figures 1b and 1c. The architecture of the molecule exhibits internal two-fold symmetry relating the two halves, termed A and B, which are each composed of a β sheet and an associated α helix. The two-fold axis passes through the middle of the molecule in a vertical direction as in the view used in Figures 1a and

Key words: actinoporin; cathion channel; equinatoxin II; membrane pore; crystal structure; soluble form

(a)

(b)

(c)

Half A   Half B

(d)

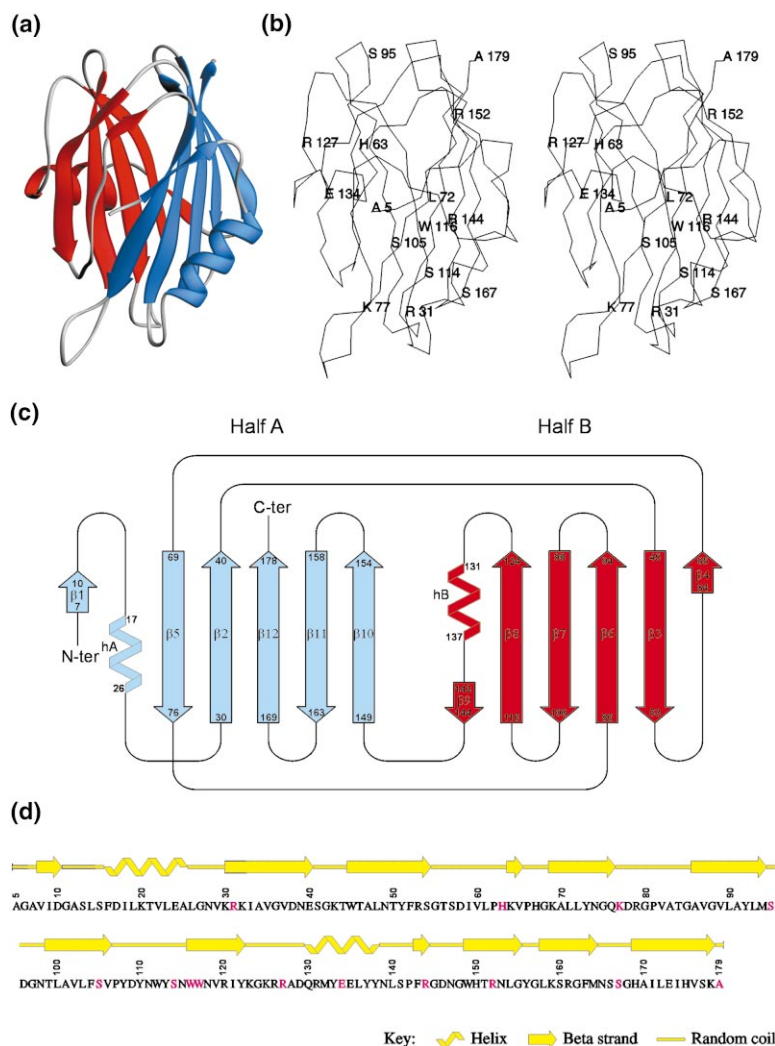Key: ∿ Helix   ▭ Beta strand   — Random coil

Figure 1. Overall Structure and Folding of Eqt II

All views shown in the figures share approximately the same up-down orientation.

(a) A ribbon representation of the EqtII monomer. Secondary structure elements of Half A are shown in cyan, elements of Half B are shown in red, and the loop regions are shown in white.

(b) A Cα plot of the structure sharing the same view as in Figure 1a. The amino acid sequence and sequence IDs are demark most of the mentioned residues.

(c) A topological diagram of the Equinatoxin II structure. β strands are labeled in the order of their appearance from the N to the C terminus. α helices are labeled according to the halves of which they are a part. The first residue of each secondary structure element is marked with its sequence ID.

(d) The sequence of EqtII, with annotated secondary structure elements on the top. The mutated residues that are referenced in the text are marked.

1b. However, only the two-fold symmetry is apparent, since the intersheet connections that are based on the differences between the mixed and antiparallel β sheet arrangements prevent any reasonable superposition of the three-dimensional structure of the two halves. (Figure 1a–c).

The interior of the β sandwich is composed of hydrophobic side chains. Each helix lies across a β sheet formation. Helix A residues lie between the short β1 strand at the edge and the β2 strand in the middle of sheet A, whereas helix B is located between two neighboring strands, β8 and β9, at the front edge of sheet B (Figures 1a and 1b). The chain of helix B is covalently attached at each end to the β sheet structure, whereas helix A is attached only on one side, where residue Lys-30 starts the β2 strand in the central region of β sheet A. The first 30 N-terminal residues of EqtII lie in a hydrophobic groove around Leu-72 on the face of β sheet A (Figure 2).

Four short β hairpin loops, two broad loops, and the C terminus of the molecule form the rather flat surface on the top of the β sheet sandwich (Figure 1). In contrast, the six loops of various lengths at the bottom of the sandwich (Figure 1) form a very uneven surface. The two loops connecting strands β5 and β6 (Lys-77– Gly85) and β7–β8 (Val-106–Asn-115) are particularly long and broad and stand out from the body of the molecule.

The EqtII molecule has a high isoelectric point (10.5). The positively charged residues are located primarily in the loop regions at the top and the bottom of the structure, whereas negatively charged residues are located in the middle of the molecule, on and close to both helices (Figure 1b). At the bottom of half A, there are charged residues in and around the loops Gly-27–Lys-32 and Lys-77–Gly-85. The former loop contains a stretch of three charged residues (Lys-30, Arg-31, and Lys-32), while at the top, on half B, the loop connecting strand β8 with helix B contains a stretch of five positively charged residues (Arg-120, Lys-123, Lys-125, Arg-126, and Arg-127). Helices A and B contain two and three negatively charged residues, respectively, with a single positively charged residue in each.

Structurally Similar Proteins

Although the β sandwich fold of EqtII is a widespread motif found in proteins of very diverse function [15], of the 21 structures that scored over the default significance level for similarity of their three-dimensional
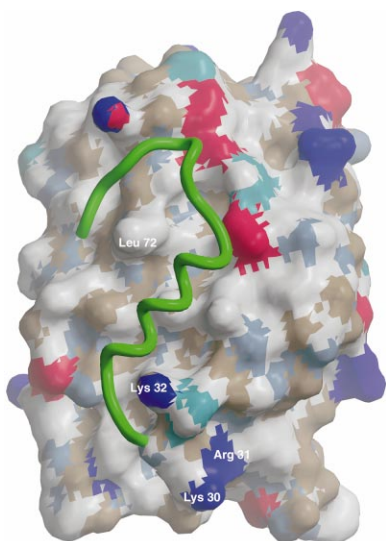
Figure 2. View Toward the Face of β Sheet A

The surface of EqtII with the 30 N-terminal residues excluded. The figure was generated with GRASP [33]. This view results from the rotation of the molecule by ∼90° about the vertical axis used in Figure 1a. These residues are shown as a green chain trace. The color coding of the surface represents the functional groups: the negatively charged carboxylic groups are red, the positively charged guanidinium and amino groups are blue, imidazole rings are cyan, the remaining oxygen atom surface is reddish, and the nitrogen atom surface is blueish. The rest of the figure is composed of the carbon atom surface and is shown in white. The figure was prepared with MAIN [30] and rendered with RENDER [34].

structures, more than half are extrinsic membrane proteins. (Extrinsic membrane proteins are proteins that attach to the membrane but are not incorporated into it.) The three most similar structures were found in thaumatin (1THV), the α subunit of the clathrin adaptor ap-2 (1QTS), and perfringolysin (protein data bank, 1PFO), with rmsd of 2.9, 3.6, and 2.8 Å for 98, 85, and 77 Cα atoms, respectively. Thaumatin and perfringolysin are connected with membrane permeabilization. Perfringolysin is a bacterial pore-forming toxin and a member of the family of thiol-activated cytolysins, which includes toxins like pneumonolysin of the highly pathogenic bacteria *Streptococcus pneumoniae*. It consists of four domains [16]. The structure of domain IV is similar to that of EqtII and is essential for interaction with the membrane. Thaumatin is not a pore- forming toxin, but it is a structural representative of the plant pathogen–related proteins (PR-5) that have pore-forming properties.

Formation of the Functional Pore

Formation of the EqtII pore is a two-step process. Initially, soluble EqtII molecules bind to the membrane. After a sufficient concentration of bound molecules is reached, pore formation follows, presumably as a consequence of the oligomerization of the 3–4 monomers [5]. Although an electron microscopy image of Sticholysin II, a closely related member of the actinoporin family, on a phospholipid monolayer film was reported, the results do not allow conclusions to be drawn about the orientation and the oligomer formation of the mem-
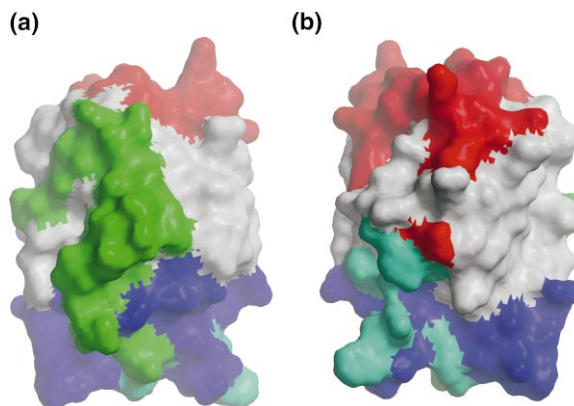

Figure 3. Location of Suggested Functionally Relevant Regions on the EqtII Surface

The region exposed to the solvent in the active, membrane-bound form is shown in red, the surface of the 30 N-terminal residues is shown in green, the surface of the loops supported by Arg-31 (Tyr-110, Lys-77, and Ser-167) are shown in blue, and the surface of the aromatic cluster is shown in cyan. The front views of sheets A and B were generated by ∼90° rotations to the left and right about the vertical axis used in Figures 1a and 1b. The views in Figures 2 and 3a are identical. The molecular surface was generated with GRASP [33], and the figure was prepared with MAIN [30] and rendered with RENDER [34].

brane-bound form [17]. Current knowledge about the mechanism of membrane pore formation and localization of crucial residues is based primarily on site-directed mutagenesis and chemical modification studies. The FT-IR spectra of the soluble and membrane-bound forms of EqtII are similar [18], suggesting that the β sandwich remains unchanged and that analogously to the previously discussed β sandwich domains of perfringolysin and thaumatin homologs (PR-5 proteins), it probably does not insert into the membrane.

Visual inspection of the crystal structure suggests that there are two parts of the chain that could adopt a different structure without disrupting the β sandwich core: the first 30 N-terminal residues of the EqtII chain, which include helix A; and helix B, which is located in the middle of the chain. Truncation of 5, 10, and 33 residues from the N terminus results in reduced hemolytic activity (89%, 31%, and 0%, respectively) compared to the wild type [19]. This suggests that despite the increased binding to the membrane that was observed, the truncated forms are less capable of functional pore formation. The EqtII form with the first 33 residues truncated does not contain Ile-33, the first residue from the N terminus, which is part of the hydrophobic core of the β sandwich. The lack of activity of this form may thus reflect a folding problem. From the structure, it is now evident that the form with the first 29 or 30 residues truncated could be used to verify that hypothesis (Figures 2 and 3, green surface). Such a form is likely to result in a protein that has the β sandwich structure intact and still binds to the membrane but exhibits no hemolytic activity. As opposed to the negative experiment based on a truncated form, a positive experiment can also be suggested. The amino acid sequence of the EqtII sequence showed that the N-termi-
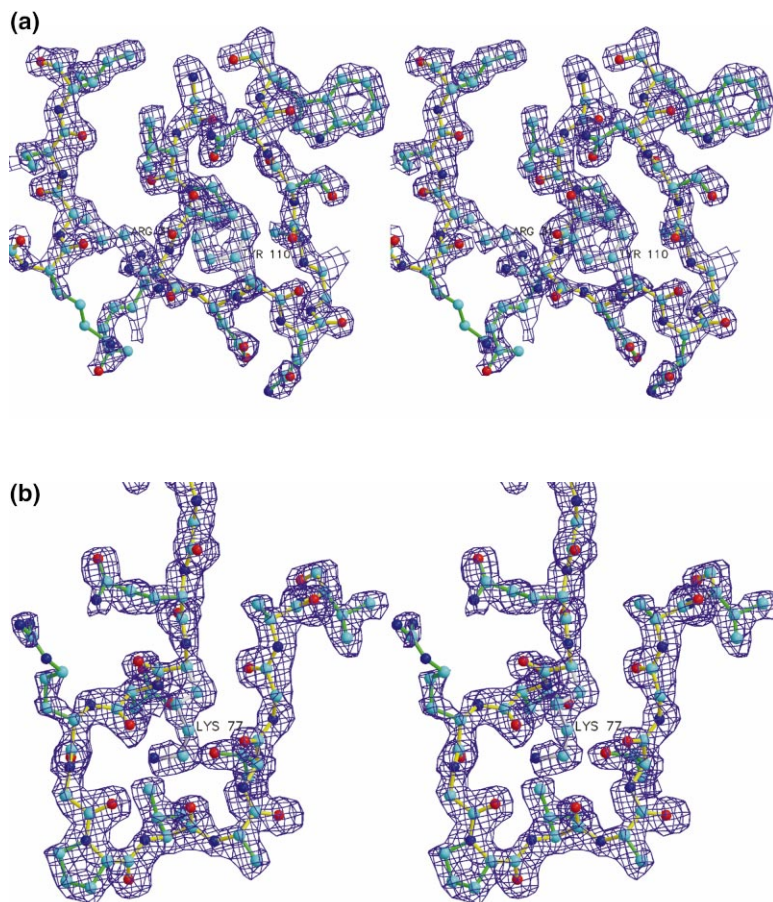
(a)

(b)

Figure 4. Structure of the Broad Loops

(a) Loop regions with the final electron density map around Arg-31/Tyr-110.

(b) Loop regions with the final electron density map around Lys-77.

The $2F_o$-F_c map contoured at 1.2 σ was prepared with MAIN [30] and rendered with RENDER [34].

nal region is the most conserved part of the protein sequence within the actinoporin family and also revealed a homology with melittin [14], a 26 residue long peptide from bee venom [20]. The structure of melittin is essentially a single α helix with a kink in the middle that is introduced by a proline residue [21]. The question to be answered is whether a 30 N-terminal residue fragment of EqtII is, like melittin, capable of membrane pore formation.

A point mutation study has shown that Trp-116 and/or Trp-117 [22] is involved in interactions with membrane lipids. While Trp-117 is buried, the side chain of Trp-116 is exposed to solvent and is positioned within a cluster of aromatic residues comprised of Tyr-133, Tyr-137, Tyr-138, Tyr-113, and Trp-112. In addition, the cysteine scan study [23] showed that the side chains of Ser-105, Ser-114, and Arg-144 located in the vicinity of the aromatic cluster also interact with a lipid membrane (Figure 3, light blue surface).

The cysteine scan revealed that the mutation of residues located within the long and broad loops connecting helix A and strand $\beta 2$ (Gly-27–Arg-31) (Figure 4a), strands $\beta 5$–$\beta 6$ (Lys-77–Val-87) (Figure 4b), and $\beta 7$–$\beta 8$ (Val-106–Asn-115), all of which protrude into the solvent, abolishes EqtII activity. The side chains of three of the mutated residues, Arg-31, Lys-77, and Ser-167, stabilize the conformation of the broad loop structures (Figures 1 and 3, dark blue surface). Restoration of the positive charge by chemical modification of the sulfohydryl

group of the Lys-77 Cys mutant with bromoethylamine results in a wild type–like active protein [18].

A site-directed mutagenesis study involving replacement of His-67, Ser-95, Arg-126, Glu-134, Arg-152, and Ala-179 (all but Glu-134 are located at the top of the structure [Figure 3, red surface]) with cysteine showed that these residues are exposed to solvent in the soluble and active form, thus excluding this region from being involved in membrane contacts or oligomerization [23].

The aromatic cluster and long loops around Arg-31 (Figure 4a) and Lys-77 (Figure 4b) are located on the opposite side of the solvent-exposed region (Figures 1 and 3). Lys-30, Arg-31, and Lys-32 are adjacent to Lys-77, and the chain enters the β sheet at Lys-30. These residues could thus contribute charges for interaction with a membrane surface and provide the base from which the 30 N-terminal residues could penetrate into a membrane.

Biological Implications

Membrane pores are crucial for normal cell functioning; however, when a cell loses control over exchange of fluids with the environment, it dies. Proteins that are capable of membrane pore formation are thus potentially extremely poisonous substances. They are used by bacteria and eukaryotes as toxins that are excreted into their surroundings for defense and predatory purposes.

Table 1. Structure Determination Statistics

Data set	Native	K₂PtCl₄	AuCl₃	Os
Space group	$P2_12_12_1$			
A (Å)	81.62	82.16	82.23	82.23
B (Å)	129.04	129.63	129.44	129.23
C (Å)	31.76	32.05	31.92	31.73
Resolution range	14.3–1.9	24.8–2.5	10.0–2.0	24.7–2.4
Unique reflections	27,057	11,921	15,789	13,138
Total Reflections	240,282	57,881	113,122	54,879
Completeness (%)	96.7	97.5	97.3	98.7
Anomalous Completeness (%)	-	85.8	81.3	93.0
R_{sym}	6.6	8.2	5.7	7.0
I/σ(I)	6.9	7.5	8.3	7.4
R_{iso}	-	30.2	15.9	15.3
Sites	-	2	3	3
Phasing Power Acentric (Centric)		1.26(0.94)	1.48(0.92)	0.94(0.80)
FOM (24.61–2.66Å)	0.45			
Reflections in refinement	26,965			
R factor (%)	19.0			
R_{free} (%)	23.5			
Average B (Å²)	16.29			
Average B main chain (Å²)	12.49			
Number of protein atoms	2,733			
Water Molecules	383			
Sulphate ions	11			
Angle rmsd (°)	1.55			
Bond rmsd (Å)	0.0086			

The crystal structure of the soluble form of EqtII from the sea anemone *Actinia equina* sheds light on the pore formation mechanism of an eukaryotic toxin. The gathered data indicates that the structure of the β sandwich motif remains unaltered upon membrane binding and oligomerization and that the 30 N-terminal residues presumably transform their structure during the process of membrane penetration. These residues are suggested to serve as a membrane anchor. Three-dimensional structural data of EqtII are now making it possible to point out the residues involved in the mechanism of membrane penetration and to unravel the residues' roles by means of site-directed mutagenesis.

Understanding the mechanism of pore formation is also of potential medical interest; specifically, properly targeted pore-forming toxins have the potential to kill infected or cancerous cells [24].

Experimental Procedures

Protein Isolation and Crystallization
Native EqtII was isolated as described previously [3]. Crystals were obtained in hanging drops containing protein (5 mg/ml), 5% isopropanol, 1.3 M ammonium sulfate, and 100 mM sodium acetate (pH 4.6) equilibrated at 20°C. The crystals belong to the $P2_12_12_1$ space group with cell parameters a = 81.62 Å, b = 129.04 Å, and c = 31.76 Å and contain two molecules per asymmetric unit.

Data Collection and Phasing
A native data set from EqtII crystals was collected at 100K on the XRD beamline of the Elettra synchrotron using a Mar345 image plate detector. The crystals were flash frozen after being dipped into a solution containing 15% glycerol in the mother liquor. Heavy atom derivatives of the protein were prepared by soaking the EqtII crystals in solutions of 10 mM AuCl₃, 10 mM K₂OsCl₆, and 10 mM K₂(CN)₆Pt. The heavy atom derivative data sets were collected using a Rigaku RU200 rotating anode X-ray source. Data processing was performed using MOSFLM [25], while intensity scaling and merging (Table 1) was done with SCALA. Heavy atom sites were located with RSPS

[26] from difference Patterson maps at 5 and 3 Å resolution [27]. Refinement of the heavy atom parameters, phase calculation, and solvent flattening of the initial MIR map were performed with SHARP and SOLOMON [28, 29].

Model Building and Refinement
Model building and electron density averaging were done using MAIN [30]. Refinement was done with MAIN [30] and XPLOR [31]. The final model (Table 1) consists of 349 residues, 383 solvent molecules, and 11 sulfate ions. Five N-terminal residues from monomer A and four from monomer B, side chains of Asn-111 and Trp-112 from monomer A, and part of the side chains of Arg-75 in both monomers were not revealed by the final electron density map. The correctness of the structure was monitored using MAIN [30]. The final refinement data and statistics are shown in Table 1. DALI [32] was used to perform a three-dimensinoal structural similarity search.

References

1. Saier, M.H., Jr. (2000). A functional-phylogenetic classification system for transmembrane solute transporters. Microbiol. Mol. Biol. Rev. *64*, 354–411.

2. Wang, Y., Chua, K.L., and Khoo, H.E. (2000). A new cytolysin from the sea anemone, *Heractis magnifica*: isolation, cDNA cloning and functional expression. Biochim. Biophys. Acta *1478*, 9–18.

3. Maček, P., and Lebez, D. (1988). Isolation and characterization of three lethal and hemolytic toxins from the sea anemone *Actinia equina*. Toxicon *26*, 441–451.

4. Maček, P. (1992). Polypeptide cytolytic toxins from sea anemones (Actiniaria). FEMS Microbiol. Immunol. *5*, 121–129.

5. Belmonte, G., Pederzolli, C., Maček, P., and Menestrina, G.

(1993). Pore formation by the sea anemone cytolysin equina-toxin II in red blood cells and model lipid membranes. J. Membr. Biol. *131*, 11–22.

6. Batista, U., Maček, P., and Sedmak, B. (1990). Thy cytotoxic and cytolytic activity of equinatoxin II from the sea anemone *Actinia equina*. Cell Biol. Int. Rep. *14*, 1013–1024.

7. Bunc, M., Drevenšek, G., Budihna, M., and Šuput, D. (1999). Effects of equinatoxin II from *Actinia equina* on isolated rat heart: the role of direct cardiotoxic effects in equinatoxin II lethality. Toxicon *37*, 109–123.

8. Gouaux, E. (1997). Channel-forming toxins: tales of transforma-tion. Curr. Opin. Struct. Biol. *7*, 566–573.

9. Shin, Y.K., Levinthal, C., Levinthal, F., and Hubbell, W.L. (1993). Colicin E1 binding to membranes: time-resolved studies of spin-labeled mutants. Science *259*, 960–963.

10. Oh, K.J., Zhan, H., Cui, C., Hideg, K., Collier, R.J., and Hubbell, W.L. (1996). Organization of diphtheria toxin T domain in bi-layers: a site-directed spin labeling study. Science *273*, 810–812.

11. Song, L., Hobaugh, M.R., Shustak, C., Cheley, S., Bayley, H., and Gouaux, J.E. (1996). Structure of staphylococcal alpha-hemolysin, a heptameric transmembrane pore. Science *274*, 1859–1866.

12. Petosa, C., Collier, R.J., Klimpel, K.R., Leppla, S.H., and Lidding-ton, R.C. (1997). Crystal structure of the anthrax toxin protective antigen. Nature *385*, 833–838.

13. Shatursky, O., et al., and Tweten, R.K. (1999). The mechanism of membrane insertion for a cholesterol-dependent cytolysin: a novel paradigm for pore-forming toxins. Cell *99*, 293–299.

14. Belmonte, G., et al., and Maček, P. (1994). Primary and second-ary structure of a pore-forming toxin from the sea anemone, *Actinia equina* L. and its association with lipid vesicles. Biochim. Biophys. Acta *1192*, 197–204.

15. Gerstein, M., and Levitt, M. (1997). A structural census of the current population of protein sequences. Proc. Natl. Acad. Sci. USA *94*, 11911–11916.

16. Rossjohn, J., Feil, S.C., McKinstry, R.K., Tweten, R.K., and Par-ker, M.W. (1997). Structure of a cholesterol-binding thio-acti-vated cytolysin and a model of its membrane form. Cell *89*, 685–692.

17. Martin-Benito, J., Gavilanes, F., de los Rios, V., Mancheno, J.M., Fernandez, J.J., and Gavilanes, J.G. (2000). Two-dimensional crystallization on lipid monolayers and three-dimensional struc-ture of sticholysin II, a cytolysin from the sea anemone *Sticho-dactyla helianthus*. Biophys. J. *78*, 3186–94.

18. Anderluh, G., Barlie, A., Potrich, C., Maček, P., and Menestrina, G. (2000). Lysine 77 is a key residue in aggregation. J. Membrane Biol. *173*, 47–55.

19. Anderluh, G., Pungerčar, J., Križaj, I., Štrukelj, B., Gubenšek, F., and Maček, P. (1997). N-terminal truncation mutagenesis of equinatoxin II, a pore-forming protein from the sea anemone *Actinia equina*. Protein Eng. *10*, 751–755.

20. Habermann, E., and Jentsch, J. (1967). Sequence analysis of melittin from tryptic and peptic degradation. Hoppe Seylers Z. Physiol. Chem. *348*, 37–50.

21. Terwilliger, T.C., and Eisenberg, D. (1982). The structure of melit-tin. J. Biol. Chem. *257*, 6016–6022.

22. Malovrh, P., Barlic, A., Podlesek, Z., Maček, P., Menestrina, G., and Anderluh, G. (2000). Structure-function studies of trypto-phan mutants of equinatoxin II, a sea anemone pore-forming protein. Biochem. J. *346*, 223–232.

23. Anderluh, G., Barlie, A., Podlesek, Z., Maček, P., Pungerear, J., Gubenšek, F., et al. (1999). Cysteine scanning mutagnesis of an eukaryotic pore-forming toxin from sea anemone: topology in lipid membranes. Eur. J. Biochem. *263*, 128–136.

24. Pederzolli, C., Belmonte, G., Dalla Serra, M., Maček, P., and Menestrina, G. (1995). Biochemical and cytotoxic properties of conjugates of transferrin with equinatoxin II, a cytolysin from a sea anemone. Bioconjug. Chem. *6*, 166–173.

25. Leslie, A.G.W. (1992). Joint CCP4 ESF-EACBM Newsletter on Protein Crystallography. (Warrington, UK: SERC Daresbury Lab-oratory).

26. Knight, S. (1989). PhD thesis, Swedish University of Agricultural Sciences, Uppsala, Sweden.

27. Collaborative Computational Project No 4. (1994). The CCP4 suite: programs for protein crystallography. Acta Crystallogr. D *50*, 760–763.

28. de La Fortelle, E., and Bricogne, G. (1997). Maximum-likelihood refinement of heavy-atom parameters in the MIR and MAD methods. In Methods Enzymology, Macromolecular Crystallog-raphy, R.M. Sweet, and C.W. Carter, Jr., eds. (New York: Aca-demic Press), pp, 472–494.

29. Abrahams, J.P., and Leslie, A.G.W. (1996). Methods used in the structure determination of bovine mitochondrial F1 ATPase. Acta Crystallogr. D *52*, 30–42.

30. Turk, D. (1992). PhD thesis, Weiterentwicklung eines programms für molekülgraphik und elektrondichte-manipulation und seine anwendung auf verschiedene protein-strukturanufklärungen. Technische Universität, München.

31. Brünger, A.T. (1993). X-PLOR Version 3.1: A System for X-ray Crystallography and NMR (New Haven, Yale University Press).

32. Holm, L., and Sander, C. (1993). Protein structure comparison by alignment of distance matrices. J. Mol. Biol. *233*, 123–138.

33. Nicholls, A., Sharp, K.A., and Honig, B. (1991). Protein folding and association: insights for the interfacial and thermodynamic properties of hydrocarbons. Proteins *11*, 281–376.

34. Merritt, E.A., and Bacon, D.J. (1997). Raster3D: photorealistic molecular graphics. Methods Enzymol. *277*, 505–524.

Accession Numbers

The coordinates are deposited in the Protein Data Bank under ac-cession number 1IAZ and were released with the date of publication.